

AB-INITIO CALCULATIONS OF OXYGEN VACANCY IN Ga₂O₃ CRYSTALS

A. Usseinov^{1*}, Zh. Koishybayeva^{1*}, A. Platonenko², A. Akilbekov¹,
J. Purans², V. Pankratov², Y. Suchikova³, A. I. Popov^{1, 2, 4*}

¹L.N. Gumilyov Eurasian National University,
2 Satpaeva Str., Nur-Sultan, KAZAKHSTAN

²Institute of Solid State Physics, University of Latvia,
8 Kengaraga Str., Riga, LV-1063, LATVIA

³Berdyansk State Pedagogical University,
4 Schmidta St., Berdyansk, 71100, UKRAINE

⁴Institute of Physics, University of Tartu,
1 W. Ostwald Str, Tartu, 50411, ESTONIA

*E-mail: usseinov_ab@enu.kz, zhanymgul.k@zerek.kz,
popov@latnet.lv

Gallium oxide β -Ga₂O₃ is an important wide-band gap semiconductor. In this study, we have calculated the formation energy and transition levels of oxygen vacancies in β -Ga₂O₃ crystal using the B3LYP hybrid exchange-correlation functional within the LCAO-DFT approach. The obtained electronic charge redistribution in perfect Ga₂O₃ shows notable covalency of the Ga-O bonds. The formation of the neutral oxygen vacancy in β -Ga₂O₃ leads to the presence of deep donor defects with quite low concentration. This is a clear reason why oxygen vacancies can be hardly responsible for n-type conductivity in β -Ga₂O₃.

Keywords: β -Ga₂O₃, ab-initio calculations, band structure, DFT, oxygen vacancy.

1. INTRODUCTION

Performance optimization of the functional properties of many advanced oxide materials depends on the control of point structural defects and also on a deep knowledge and understanding of their various properties and characteristics [1]–[9]. Special attention has recently been paid to gallium oxide $\beta\text{-Ga}_2\text{O}_3$ as a very promising candidate for optoelectronic devices operating at short wavelengths. Due to its wide band gap and possible modulation of optical properties by synthesis methods and doping impurities, it is a very attractive material for use in different optoelectronic devices, as well as in photocatalysis, optical fibres and scintillators [10]–[17].

One of the most important areas of both research and application is the control of electrical conductivity through doping of the material. Traditionally, in many oxygen-containing materials, oxygen vacancies (V_{O}) are considered a source of electrical conductivity [1], [2], [10], [18], [19]. How-

ever, recent density functional theory (DFT) calculations of Ga_2O_3 have shown that oxygen vacancies do not play a key role in conductivity [20]. At the same time, already small amounts of unintentional donors, like hydrogen, completely change the electronic structure and explain the observed activation energy of conductivity (1.7 eV) [20]. In this regard, DFT calculations play an exceptional role in understanding this fundamental issue through the study of the electronic structure and defects energetics.

In this paper, we present the results of *ab-initio* calculations of a pure and defective (with one oxygen vacancy) $\beta\text{-Ga}_2\text{O}_3$ crystal using the hybrid B3LYP exchange-correlation functional and the LCAO approximation. To describe the effect of oxygen vacancy onto electronic and conductivity properties, the charge transition levels as function of the Fermi energy have been calculated.

2. COMPUTATIONAL SET AND Ga_2O_3 CRYSTAL STRUCTURE

Large-scale *ab initio* calculations have been performed using a linear combination of atomic orbital method within the density functional theory (LCAO-DFT) approach. The hybrid B3LYP [21] functional has been used, allowing us to perform very accurate calculations of the band gap, unlike the standard LDA or GGA-type functionals. The basic sets for Ga and O atoms have been taken from Ref. [22], [23], respectively. The integration over the Brillouin zone in the reciprocal space has been performed within a $4\times 4\times 4$ Pack-Monkhorst grid [24]. Effective atomic charges have been estimated using the Mulliken popula-

tion analysis [25].

The $\beta\text{-Ga}_2\text{O}_3$ unit cell is shown in Fig. 1, where $a\perp c$, $b\perp c$, and the angle between a and c axes is 104° . The lattice parameters are $a = 12.19 \text{ \AA}$, $b = 3.05 \text{ \AA}$, and $c = 5.82 \text{ \AA}$. By symmetry, there are two distinct Ga sites, labelled Ga(1) and Ga(2) (Fig. 1). The Ga(1) atoms are bonded to four neighbouring O atoms in a (roughly) tetrahedral arrangement. The Ga(2) atoms are in an octahedral environment and bind to six neighbouring O atoms. The O atoms have three distinct sites: O(1) and O(2) bind to three Ga atoms, while O(3) binds to four Ga atoms. The Ga–O bond lengths range from

1.8 to 2.1 Å.

To simulate an oxygen vacancy, a periodic model of the extended unit cell of the crystal – a supercell – with an expansion matrix of $2 \times 2 \times 2$ and containing 80 atoms has been used.

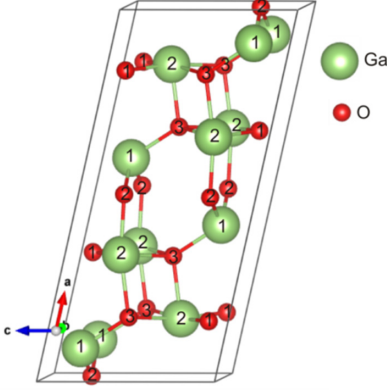


Fig. 1. Schematic representation of crystal structure of monoclinic β -Ga₂O₃. Unique positions of Ga/O atoms in the lattice are designated.

Further, we have calculated the bulk properties of pure Ga₂O₃ obtaining good agreement with the experimental data (Table 1). The optimized lattice parameters a and c slightly overestimate those obtained in experiments. The error in the estimate of band gap energies obtained using hybrid calculations has been found to be much smaller than the error in standard GGA-PBE or Hartree-Fock calculations (resulted in a huge underestimate/overestimate of the band gap). Proper estimate of band gap is an important point, since the correct description of formation energy depends on it. Mulliken's analysis showed a slight difference in the ionic charge on atoms with different positions in the crystal, which was associated with the anisotropy of the electronic properties [$q(\text{Ga1}) + 1.48e$, $q(\text{Ga2}) + 1.58e$, $q(\text{O1}) = - 0.994e$, $q(\text{O2}) = - 0.997e$, $q(\text{O3}) = - 0.079e$], as well as a considerable covalency of the Ga-O bonding ($\sim 0.2e$).

Table 1. Bulk Properties of Pure β -Ga₂O₃ as Calculated by Means of DFT-LCAO Method

	HF	GGA-PBE	B3LYP	Exp [10]
a , Å	12.19	12.34	12.34	12.12÷12.34
b , Å	3.05	3.11	3.09	3.03÷3.04
c , Å	5.82	5.90	5.87	5.80÷5.87
E_g , eV (direct/indirect)	13.8	2.36/2.3	4.49/4.45	4.4÷5

3. FORMATION ENERGIES AND TRANSITION LEVELS

As it is known, formation energy of defect D with charge q in system X is

defined as:

$$E_f = E_{tot}(D) - E_{tot}(X) + \sum_i n_i \mu_i + q(E_F + E_V) + E_{corr}, \quad (1)$$

where $E_{tot}(D)$ and $E_{tot}(X)$ are the total energies of the system with and without a defect, n_i represents the number of atoms of the element i that are removed from the

system when a defect is formed (a negative value for n_i means the addition of atoms), μ_i is the chemical potential of element i , it is the energy of atoms that are removed

(or added) into the system when a defect is formed. The study is performed for dopant-rich condition, using molecular O_2 as a dopant source in the gas phase. The fourth term $q(E_F+E_V)$ is a change in the electron energy due to the exchange of electrons and holes with the carrier reservoirs. E_F+E_V is the Fermi energy relative to the maximum of the valence band of a defect-free system. E_{corr} term includes energy offset correction [26] and first-order Makov-Payne correction [27].

$$1/2\mu(O_2) + 1/3 E_f(Ga_2O_3) < \mu_o < 1/2\mu(O_2).$$

To determine the charge state transition levels for various defects, we used the approximation described by Lany and Zunger [28], based on previous studies by

$$\begin{aligned} E_{tot}(D, q) - E_{tot}(X) + \sum_i n_i \mu_i + q \left(\varepsilon \left(\frac{q}{q'} \right) + E_V \right) \\ = E_{tot}(D, q') - E_{tot}(X) + \sum_i n_i \mu_i + q' \left(\varepsilon \left(\frac{q}{q'} \right) + E_V \right), \end{aligned}$$

thus

$$\varepsilon(q/q') = \frac{E(D, q') - E(D, q)}{q - q'} - E_V. \quad (2)$$

The zero energy reference is set at the top of the valence band, $E_V=0$. We have considered cases in which an electronic charge is added to the system, i.e., the state q' cor-

To calculate chemical potentials included in Eq. (1), we take the O_2 molecule (oxygen-rich conditions) and the Ga metal (oxygen-poor conditions) as limiting phases. Combining the expressions $\mu_o < 1/2\mu(O_2) = 1/2E_{tot}(O_2)$; $\mu_{Ga} < \mu_{Ga-metal} = E_{tot}(Ga)$; $2\mu_{Ga} + 3\mu_o = \mu(Ga_2O_3) = E_{tot}(Ga_2O_3)$ and the formation energy of the compound $E_f(Ga_2O_3) = E_{tot}(Ga_2O_3) - 2\mu_{Ga-metal} - 3/2\mu(O_2)$, one gets the range of μ_o , the chemical potential of oxygen in gallium oxide:

Scherz and Scheffler [29], stating that the transition level is the Fermi energy, at which the formation energy of a charged defect is equal to that of a neutral defect:

responds to a state with an extra electron, $q+1e$: this corresponds to a transition from a neutral state to a negatively charged state, $\varepsilon(0/-1)$.

4. RESULTS AND DISCUSSION

The formation energy for oxygen vacancies in three different crystallographic positions (see Fig.1) is shown in Fig. 2. Neutral V_o has the lowest energy on the O(3) site. The bend of the curve corresponds to

the transition of the defect charge state. As formation energies for all types of V_o in 1+ charge state are around 2.5 eV, the oxygen vacancy is an example of a negative-U defect, where the 1+ charge state is unsta-

ble. At low Fermi energies, the 2+ charge state becomes more preferable, whereas when Fermi level is high, the neutral state becomes the most stable. For an oxygen-poor conditions, we obtain $\epsilon(2+/0)=4$ eV for O(1), $\epsilon(2+/0)=3.8$ eV for O(2), $\epsilon(2+/0)=3.1$ eV for O(3). Under an oxygen-rich condition, formation energy increases by ~ 2.76 eV. Transition levels are equal or more than 1eV below CB. The amount of thermal energy required to promote an electron from the defect level to the CB is much greater than the room temperature; therefore, oxygen vacancies are *deep donors* and cannot serve as the effective source of the electron charge. Hence, oxygen vacancies cannot be responsible for n-type conductivity in Ga_2O_3 . However, they can compensate acceptors by donating their electrons. As acceptor doping increases, the Fermi level is pushed down toward the VB. This reduces the formation energy for oxygen vacancies. At some point, the formation energy gets small such that the Fermi level is prevented from going any lower.

On the other hand, as shown earlier, hydrogen can be easily accumulated in a crystal due to a small migration barrier of 0.34 eV [30]. After penetrating into a crystal, hydrogen can occupy many interstitial sites (H_i) nearby to oxygen atoms with creating of O-H bounds, and also penetrate into

oxygen vacancies (H_o). In all cases, hydrogen acts as a *shallow donor*. It is important to note that similar behaviour of hydrogen as a donor impurity appears in other oxide materials (ZnO , SnO_2 , In_2O_3) and thus has some generality in these properties [10], [30]. There is some experimental support to the fact that hydrogen may be a shallow donor in $\beta\text{-Ga}_2\text{O}_3$ from experiments on its muonium counterpart and from electron paramagnetic resonance of single-crystal samples [31], [32]. Therefore, we believe that hydrogen is more preferable as a source of unintentional background n-type conductivity.

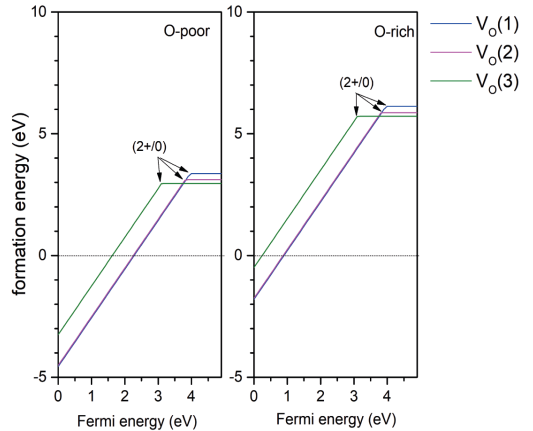


Fig. 2. Formation energies of V_o in $\beta\text{-Ga}_2\text{O}_3$ plotted against the Fermi energy for (a) oxygen-poor and (b) oxygen-rich conditions. For V_o , the three different vacancies are denoted $V_o(1)$, $V_o(2)$ and $V_o(3)$ as shown in Fig. 1.

5. CONCLUSIONS

In this study, we have calculated the formation energy and transition levels of oxygen vacancies in Ga_2O_3 crystal using the B3LYP hybrid exchange-correlation functional within the LCAO-DFT approach. The electronic charge redistribution in perfect Ga_2O_3 shows notable covalency of the Ga-O bonds. Formation of the oxygen vacancy in $\beta\text{-Ga}_2\text{O}_3$ leads to the presence

of deep donor defects. That is why neutral oxygen vacancies can be hardly responsible for n-type conductivity in $\beta\text{-Ga}_2\text{O}_3$ accompanied by their quite high formation energy. In this respect, In this regard, we assume that the observed n-type conductivity in gallium oxide is due to the presence of interstitial and substituting hydrogen impurities in the crystal lattice.

ACKNOWLEDGEMENTS

The research has been funded by the Science Committee of the Ministry of Education and Science of the Republic of Kazakhstan (Grant No. AP08856540). J. Purans and A.I. Popov acknowledge the ERAF project 1.1.1.1/20/A/057 “Functional Ultrawide Bandgap Gallium Oxide and Zinc Gallate Thin Films and Novel

Deposition Technologies”.

The Institute of Solid State Physics, University of Latvia (Latvia) as the Centre of Excellence has received funding from the European Union’s Horizon 2020 Framework Programme H2020-WIDESPREAD-01-2016-2017-Teaming Phase2 under grant agreement No. 739508, project CAMART2.

REFERENCES

1. Shluger, A. (2020). Defects in Oxides in Electronic Devices. *Handbook of Materials Modeling: Applications: Current and Emerging Materials*, 1013–1034.
2. Maier, J. (2003). Complex Oxides: High Temperature Defect Chemistry vs. Low Temperature Defect Chemistry. *Physical Chemistry Chemical Physics*, 5 (11), 2164–2173.
3. Lee, D., Park, J. W., Cho, N. K., Lee, J., & Kim, Y. S. (2019). Verification of Charge Transfer in Metal-Insulator-Oxide Semiconductor Diodes via Defect Engineering of Insulator. *Scientific Reports*, 9 (1), 10323.
4. Popov, A. I., Kotomin, E. A., & Maier, J. (2010). Basic Properties of the F-Type Centers in Halides, Oxides and Perovskites. *Nuclear Instruments and Methods in Physics Research Section B: Beam Interactions with Materials and Atoms*, 268 (19), 3084–3089.
5. Kozlovskiy, A., Kenzhina, I., Kaikanov, M., Stepanov, A., Shamanin, V., Zdorovets, M., & Tikhonov, A. (2018). Effect of Electronic Modification on Nanostructures Stability to Degradation. *Materials Research Express*, 5 (7), 075010.
6. Rusevich, L. L., Kotomin, E. A., Zvejnieks, G., & Popov, A. I. (2020). *Ab Initio* Calculations of Structural, Electronic and Vibrational Properties of BaTiO₃ and SrTiO₃ Perovskite Crystals with Oxygen Vacancies. *Low Temperature Physics*, 46 (12), 1185–1195.
7. Zhumatayeva, I. Z., Kenzhina, I. E., Kozlovskiy, A. L., & Zdorovets, M. V. (2020). The Study of the Prospects for the Use of Li_{0.15}Sr_{0.85}TiO₃ Ceramics. *Journal of Materials Science: Materials in Electronics*, 31 (9), 6764–6772.
8. Chornaja, S., Sproge, E., Dubencovs, K., Kulikova, L., Serga, V., Cvetkovs, A., & Kampars, V. (2014). Selective Oxidation of Glycerol to Glyceraldehyde over Novel Monometallic Platinum Catalysts. *Key Engineering Materials*, 604, 138–141.
9. Eglitis, R., Popov, A. I., Purans, J., & Jia, R. (2020). First Principles Hybrid Hartree-Fock-DFT Calculations of Bulk and (001) Surface F Centers in Oxide Perovskites and Alkaline-Earth Fluorides. *Low Temperature Physics*, 46 (12), 1206–1212.
10. Pearton, S. J., Yang, J., Cary IV, P. H., Ren, F., Kim, J., Tadjer, M. J., & Mastro, M. A. (2018). A Review of Ga₂O₃ Materials, Processing, and Devices. *Applied Physics Reviews*, 5 (1), 011301.
11. Higashiwaki, M., Sasaki, K., Murakami, H., Kumagai, Y., Koukitu, A., Kuramata, A., ... & Yamakoshi, S. (2016). Recent Progress in Ga₂O₃ Power Devices. *Semiconductor Science and Technology*, 31 (3), 034001.

12. Luchechko, A., Vasylytsiv, V., Kostyk, L., Tsvetkova, O., & Popov, A. I. (2019). Shallow and Deep Trap Levels in X-Ray Irradiated β -Ga₂O₃: Mg. *Nuclear Instruments and Methods in Physics Research Section B: Beam Interactions with Materials and Atoms*, 441, 12-17.
13. Drozdowski, W., Makowski, M., Witkowski, M. E., Wojtowicz, A. J., Schewski, R., Irmscher, K., & Galazka, Z. (2020). Semiconductor Scintillator Development: Pure and Doped β -Ga₂O₃. *Optical Materials*, 105, 109856.
14. Zhao, M., Tong, R., Chen, X., Ma, T., Dai, J., Lian, J., & Ye, J. (2020). Ellipsometric Determination of Anisotropic Optical Constants of Single Phase Ga₂O₃ Thin Films in its Orthorhombic and Monoclinic Phases. *Optical Materials*, 102, 109807.
15. Xu, C. X., Liu, H., Pan, X. H., & Ye, Z. Z. (2020). Growth and characterization of Si-doped β -Ga₂O₃ films by pulsed laser deposition. *Optical Materials*, 108, 110145.
16. Feng, B., Li, Z., Cheng, F., Xu, L., Liu, T., Huang, Z., ... & Ding, S. (2020). Investigation of β -Ga₂O₃ Film Growth Mechanism on c-Plane Sapphire Substrate by Ozone Molecular Beam Epitaxy. *Physica Status Solidi (a)*, 2000457. <https://doi.org/10.1002/pssa.202000457>
17. Alhalaili, B., Bunk, R. J., Mao, H., Cansizoglu, H., Vidu, R., Woodall, J., & Islam, M. S. (2020). Gallium Oxide Nanowires for UV Detection with Enhanced Growth and Material Properties. *Scientific Reports*, 10, 21434. <https://doi.org/10.1038/s41598-020-78326-x>
18. Yin, W. J., Wei, S. H., Al-Jassim, M. M., & Yan, Y. (2011). Prediction of the Chemical Trends of Oxygen Vacancy Levels in Binary Metal Oxides. *Applied Physics Letters*, 99 (14), 142109.
19. Biswas, P., Ainabayev, A., Zhussupbekova, A., Jose, F., O'Connor, R., Kaisha, A., ... & Shvets, I. V. (2020). Tuning of Oxygen Vacancy-Induced Electrical Conductivity in Ti-Doped Hematite Films and its Impact on Photoelectrochemical Water Splitting. *Scientific Reports*, 10 (1), 7463. <https://doi.org/10.1038/s41598-020-64231-w>
20. Zacherle, T., Schmidt, P. C., & Martin, M. (2013). *Ab Initio* Calculations on the Defect Structure of β -Ga₂O₃. *Physical Review B*, 87 (23), 235206.
21. Beck, A. D. (1993). Density-Functional Thermochemistry. III. The Role of Exact Exchange. *Journal of Chemical Physics*, 98 (7), 5648–6.
22. Pandey, R., Jaffe, J. E., & Harrison, N. M. (1994). *Ab Initio* Study of High Pressure Phase Transition in GaN. *Journal of Physics and Chemistry of Solids*, 55 (11), 1357–1361.
23. Towler, M. D., Allan, N. L., Harrison, N. M., Saunders, V. R., Mackrodt, W. C., & Apra, E. (1994). *Ab Initio* Study of MnO and NiO. *Physical Review B*, 50 (8), 5041.
24. Monkhorst, H. J., & Pack, J. D. (1976). Special Points for Brillouin-Zone Integrations. *Physical Review B*, 13 (12), 5188.
25. Mulliken, R. S. (1955). Electronic Population Analysis on LCAO–MO Molecular Wave Functions. II. Overlap Populations, Bond Orders, and Covalent Bond Energies. *Journal of Chemical Physics*, 23 (10), 1841–1846.
26. Bailey, C. L., Liborio, L., Mallia, G., Tomić, S., & Harrison, N. M. (2010). Calculating Charged Defects Using CRYSTAL. *Journal of Physics: Conference Series*, 242 (1), 012004.
27. Makov, G., & Payne, M. C. (1995). Periodic Boundary Conditions in *Ab Initio* Calculations. *Physical Review B*, 51 (7), 4014.
28. Lany, S., & Zunger, A. (2008). Assessment of Correction Methods for the Band-Gap Problem and for Finite-Size Effects in Supercell Defect Calculations: Case Studies for ZnO and GaAs. *Physical Review B*, 78 (23), 235104.
29. Scherz, U., & Scheffler, M. (1993). Density-Functional Theory of sp-Bonded Defects in III/V Semiconductors. *Semiconductors and Semimetals*, 38, 1–58.

30. Varley, J. B., Weber, J. R., Janotti, A., & Van de Walle, C. G. (2010). Oxygen Vacancies and Donor Impurities in β -Ga₂O₃. *Applied Physics Letters*, 97 (14), 142106.
31. King, P. D. C., McKenzie, I., & Veal, A. T. (2010). Observation of Shallow-Donor Muonium in Ga₂O₃: Evidence for Hydrogen-Induced Conductivity. *Applied Physics Letters*, 96 (6), 062110.
32. King, P. D. C., & Veal, T. D. (2011). Conductivity in Transparent Oxide Semiconductors. *Journal of Physics: Condensed Matter*, 23 (33), 334214.